Circular Array of Endfire Yagi-Uda Monopoles with A Full 360° Azimuthal Beam Scanning

Yubo Wen, Pei-Yuan Qin, Geng-Ming Wei, and Richard W. Ziolkowski

***Abstract*—A multi-port circular array of endfire Yagi-Uda monopoles with a full beam coverage of the azimuth plane is developed in this communication. The known issue that a vertical monopole antenna on a finite-sized horizontal ground plane radiates an elevated beam is investigated. It is demonstrated that this effect can be mitigated by inserting resonant structures, i.e., slots, into the ground plane to redirect the radiated beam back to the horizontal direction. An endfire monopole-based Yagi-Uda antenna is then developed that radiates a directed endfire beam. A multi-port circular array of these antennas is optimized to provide a beam coverage over the full 360° azimuthal plane. A sector of this circular array of monopole-based Yagi-Uda antennas was simulated, fabricated and measured to verify the concepts. Good agreement between the simulated and measured results is confirmed.**

***Index Terms*—Beam scanning, circular array, finite ground plane, monopole array, resonant slots, Yagi-Uda antennas**

I. Introduction

Beam scanning or multi-beam antennas that provide a 360° full azimuthal coverage have attracted more and more attention because they have applications in a wide variety of electronic systems, e.g., cognitive radios, direction-of-arrival estimation and cellular base stations. Beam scanning antennas can serve multiple users at different times by dynamically changing the directions at which their beams point. Multi-beam arrays that are fed by multiple ports can provide multiple concurrent, yet independent beams to enable multi-point-to-multi-point communications.

A general method to achieve beam scanning with a full 360° azimuthal coverage is to employ a circular antenna array with a reconfigurable feed network which has multiple input ports. These antennas can radiate a single beam by energizing one port or multiple beams by exciting multiple ports simultaneously. By activating different sectors of a circular array, beams can be radiated towards a particular set of directions. A full 360° azimuthal coverage has been achieved in several reported systems. For instance, an eight-port fed, tightly coupled slot antenna array was presented in [1] that achieved a maximum gain of 5.2 dBi in its endfire direction. A six-element circular patch array was developed in [2] that achieved a maximum gain of 8.45 dBi. A four-element dipole array was presented in [3] that had a maximum gain of 5.4 dBi. A six-element dipole circular array was developed in [4] that had a maximum gain of 3.12 dBi.

Electronically steerable parasitic array radiators (ESPARs) [5]-[10] and active frequency-selective surface (AFSS) [11]-[13] based arrays are also capable of a full 360° coverage of the azimuthal plane. The ESPAR is a classic antenna that was developed to facilitate beam scanning along the azimuthal plane. Some of the original key concepts and interesting designs are discussed in [5]. A circular array of monopoles with both active and passive elements was proposed in [7]. A dual-band ESPAR was presented in [8]. However, these types of antennas are less flexible. Because they have only one driven radiator, they can only achieve a single steered beam rather than being able to radiate multiple beams.

The authors are with the Global Big Data Technologies Centre (GBDTC), University of Technology Sydney (UTS), Ultimo, NSW 2007, Australia

It is found that all of these beam scanning and multi-beam arrays have achieved a realized gain that is below 10 dBi. This limitation is mainly attributed to the fact that the radiator associated with each beam is either a single slot/patch/dipole or a small array of them. An interesting method to achieve a full 360° azimuthal coverage with a high gain is to use an array driven with multipole ports to excite a high-impedance surface or metasurface. The high-impedance surface developed in [14] was arranged into four sectors and fed with 28 ports. Each sector produced a steered beam within its 90° quadrant and attained a maximum measured gain of 16 dBi. Furthermore, a single-layered annular surface plasmon polariton (SPP)-based leaky-wave antenna was developed in [15] that provided a 270° scanning over the azimuthal plane with a maximum gain of 19.7 dBi. The beam scanning was achieved by sweeping the operating frequency. However, the main beam direction was elevated to 46° above the azimuthal plane.

A monopole-based Yagi-Uda circular array is a very simple technology that can achieve a full 360° azimuthal scan with a high gain [16]. However, the main beam direction of the array with its finite-sized ground plane is also elevated above it as a consequence of the fields radiated by the non-trivial currents existing on its edges [6], [17]. This is usually undesirable since it reduces the terrestrial coverage. This disadvantage limits the applications of such arrays. A very early design that used a resonant slot in a flange attached to the ground plane in order to modify the radiation pattern of a Yagi-Uda linear array was introduced in [18]. The purpose of the slot was to remove an interference null by suppressing the foreground reflection. Recently, one way to enhance the endfire performance characteristics of a monopole-based array is to employ a skirted ground structure [6]. The height of the skirt affects the main beam direction. A skirt that is nearly a quarter wavelength in height will enable the beam to be pointed along the horizontal direction. Nevertheless, the size of the ground plane in the design is half a wavelength. Moreover, the feasibility of this method on a large ground plane was not considered. Another way is to place a reflector on top of the monopole antenna to make the beam directed towards the endfire direction, but the profile of the antenna becomes much higher [17].

In this communication, we report the development of an innovative monopole-based Yagi-Uda endfire antenna. Resonant slots are inserted into its ground plane; they mitigate the fields radiated by it. This configuration enables endfire beams which are radiated along the horizontal plane. Furthermore, a full 360° azimuthal scanning is achieved with a maximum realized gain over 12 dBi by forming a circular array with 18 of these endfire antennas. It is noted that a planar microstrip Yagi-Uda antenna [19], [20] can also achieve endfire performance along the azimuthal plane. However, because the driven dipole is printed on the azimuthal plane and is a half wavelength long, a circular array of planar microstrip Yagi-Uda antennas will have less beam resolution than a compact monopole array, whose radiators are perpendicular to it.

The rest of the communication is organized as follows. The operating mechanisms of the developed monopole antenna are described in Section II. The monopole-based Yagi-Uda circular array and its beam scanning abilities are presented in Section III. The

simulated and measured results for a single sector of the circular array are given in Section IV. The paper concludes in Section V.

II. Monopole Antenna with an Endfire Radiation

It is well known that if a monopole is mounted perpendicular to an infinite ground plane, it will radiate an omnidirectional pattern whose maximum direction is along that horizontal plane. However, if the ground plane is finite in size, the main beam direction will be substantially elevated above that horizontal plane. This negative feature is mainly due to the fields radiated by the currents that the monopole fields induce on the ground plane.

We have developed a finite-sized monopole-based antenna whose maximum beam direction is along the horizontal plane. The configurations of the reference (Ref.) monopole antenna and our innovative design are shown in Figs. 1(a) and 1(b), respectively. The differences between the two systems are the four resonant slots etched in the ground plane in Fig. 1(b); they are more clearly detailed in Fig. 1(c). The length of the slot is 0.42 λ_0, λ_0 being the free space wavelength of the operating frequency. The width of the slot is 0.015 λ_0. The four slots are not connected end to end. There is a small gap, 0.0075 λ_0 wide, between the ends of each slot. The length of the monopole in both systems is $\lambda_0/4$. The length and the width of the ground plane of both antennas are selected to be λ_0 simply for comparison purposes. It will be shown later that this resonant slot method is suitable to any finite-sized ground plane. Note that arc shaped slots are also capable of eliminating the current on the ground and redirecting the beam to the horizontal direction. The rectangular slots were chosen for our design and prototype simply because they were the easiest ones to fabricate.

We first present the currents of these two monopoles in order to show the effects of the slots on the radiation patterns of the monopole alone. Those of the bare monopole are given in Fig. 2(a); those of the monopole with the slots are given in Fig. 2(b). They were obtained using FEKO [21].

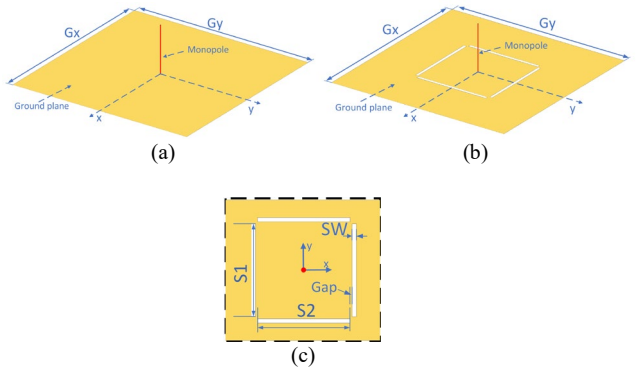

Fig. 1. Monopole-based antennas. Isometric view of the (a) Ref. monopole and (b) the monopole with the slots. (c) Top view of the slots in (b). The lengths of the ground plane along the x- and y- axes are denoted by Gx and Gy, respectively. The slot length S1 = S2 = 0.42 λ_0, slot width SW = 0.015 λ_0 and slot Gap = 0.0075 λ_0.

The currents on the edges and a majority of the ground plane when the slots are present in Fig. 2(b) are significantly smaller than those in Fig. 2(a) when they are not. As a consequence, the fields radiated from the ground plane are significantly reduced when the slots are present. Thus, there are minimal additional fields impacting those of the monopole, which facilitates the overall fields being radiated along the horizontal direction. It must be noted that there are strong currents around the resonant slot structures. However, as indicated by their directions (black arrows), the currents near the slots essentially cancel each other. There are no field components from them to elevate the pattern off from the horizontal plane on which they lie.

The resonant slot structures also act to minimize the currents on the ground plane away from the slots as shown in Fig. 2(b). Therefore, a larger ground plane will not lead to fields that would lift the monopole fields away from the horizontal plane. In fact, the resonant slot structures would also perform a similar function for an arbitrarily shaped ground plane.

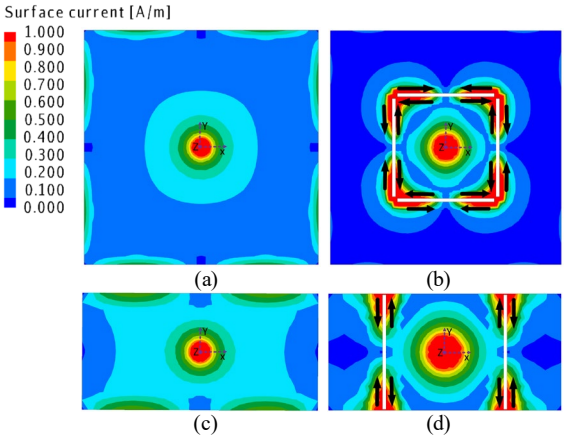

Fig. 2. Magnitude of the currents on the ground for the Ref. monopole and the monopole with slots. Gx = λ_0. (a), (b): Gy = λ_0. (c), (d): Gy = 0.5 λ_0.

When one dimension of the ground plane is reduced small enough, the slots perpendicular to this direction are not needed. For example, when the width of the ground plane Gy is reduced to 0.5 λ_0, the slots along the x-axis are not required because the currents on the ground plane away from the y-directed slots are small. The length of the remaining slots was optimized to be 0.49 λ_0 to minimize the fields radiated from the ground plane. The overall current distribution is shown in Fig. 2(d). In contrast, the current distribution of the Ref. monopole antenna with this reduced-size ground plane is given in Fig. 2(c). Comparing Figs. 2(c) and 2(d), the currents on the ground plane along the x-axis have indeed been reduced significantly for the monopole with slots. Moreover, the currents around the slots still cancel each other.

The radiation patterns of these Ref. monopole and monopole with slots cases are presented in Fig. 3. The peaks of the Ref. monopole cases are clearly elevated substantially above their ground planes. In contrast, the monopole cases with the slots have their radiation peaks along the horizontal direction. These results clearly demonstrate that by inserting resonant slots into the ground plane near the monopole, the fields radiated by the ground plane are reduced significantly and the peaks of the antenna's overall radiation pattern become horizontally directed.

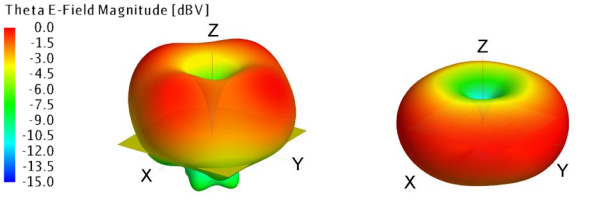

(a) Ref. case, Gx = λ_0, Gy = λ_0. (b) Slot case, Gx = λ_0, Gy = λ_0.

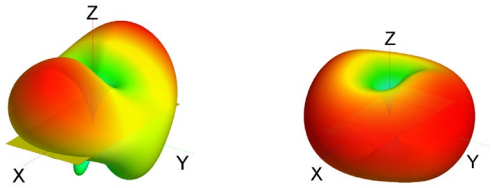

(c) Ref. case, Gx = λ_0, Gy = 0.5 λ_0. (d) Slot case, Gx = λ_0, Gy = 0.5 λ_0.

Fig. 3. Radiation patterns of the Ref. monopole and the monopole with slots.

III. Monopole-Based Yagi-Uda Antenna with Slots

Based on the developed monopole antenna with its slot structures, we have designed a monopole-based Yagi-Uda antenna whose main beam is pointed along its endfire direction. A typical Yagi-Uda antenna with no ground plane consists of a reflector, a driven dipole and several directors. It radiates an endfire beam. On the other hand, a monopole-based Yagi-Uda antenna without any slot structures radiates an elevated main beam. We employ the resonant slot approach developed for the single monopole antenna to suppress the fields radiated by the ground plane in the array version. Since the standard Yagi-Uda antenna has a directive beam with a very small backlobe, only one resonant slot per element is actually needed to implement the strategy instead of four surrounding each monopole.

Three monopole-based Yagi-Uda antennas are shown in Fig. 4. Each has its array oriented along the x-axis. The lengths of all of their elements are selected to have their main beam be pointed along the +x-axis at 3 GHz [22]. The antenna in Fig. 4(a) is the Ref. case without any slots. The antenna in Fig. 4(b) is the rectangular slot (RS) version of modified Yagi-Uda antenna, and Fig. 4(c) is the I-shaped slot (IS) version.

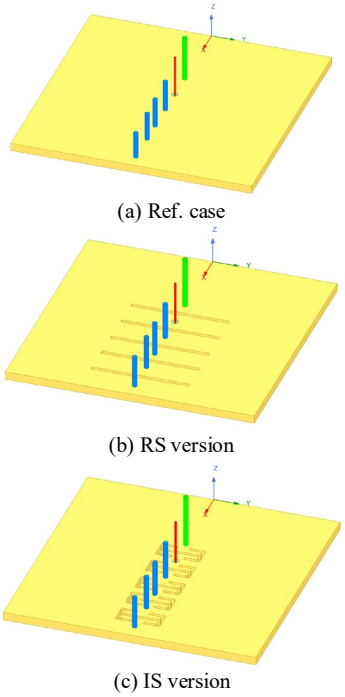

(a) Ref. case

(b) RS version

(c) IS version

Fig. 4. Monopole based Yagi-Uda antennas with a square ground plane.

The optimized parameters of the array design are illustrated in Fig. 5(a). The slots of the two cases are presented in Fig. 5 (a) and (b). The dimensions of each parameter are given in the caption of Fig. 5. The radius of the cross section of reflectors and directors are 1.5 mm, while it is 0.65 mm for the driver, which is fabricated by extending the inner conductor of the coaxial line. The resonant rectangular slots in Figs. 4(b) and 5(a) are 0.59 λ_0 long. The resonant I-shaped slots in Figs. 4(c) and 5(b) are much smaller, being only 0.265 λ_0 long.

These three monopole-based Yagi-Uda antennas were simulated using the commercial software – ANSYS Electromagnetics Suite (HFSS), version 19 [23]. Their simulated realized gain patterns at 3.0 GHz and their maximum realized gains as a function of the source frequency are compared in Figs. 6(a) and 6(b), respectively. It is found in Fig. 6(a) that the main beam direction of the Ref. antenna is noticeably elevated around 15° above the ground plane. On the other hand, those of the two slot-based cases are pointed along the +x-axis (θ=90°), i.e., along the horizontal direction. Moreover, both slot-based antennas show an improvement of the maximum gain when compared to the Ref. case of about 3.0 dB at 3.0 GHz.

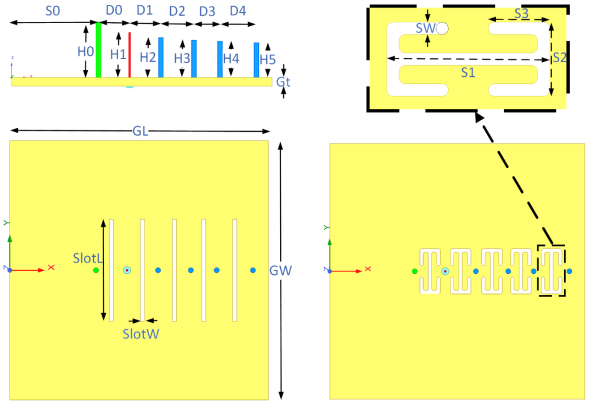

(a) RS (b) IS

Fig. 5. Monopole-based Yagi-Uda antennas having slots in their ground planes. Optimized design parameters (Dimensions in mm): *Shared values*: GL=150, GW=150, Gt=5, S0=50, D0=18, D1=18, D2=19, D3=15, D4=21, D5=21. *Ref. Yagi-Uda Antenna:* H0=29, H1=26, H2=20, H3=19, H4=18, H5=17. *RS version*: H0=32, H1=26, H2=23, H3=21.5, H4=21, H5=20, Slot L=59, Slot W=2. *IS version*: H0=32, H1=26, H2=23, H3=21.5, H4=21, H5=20, S1=26.5, S2=12, S3=10, SW=2.

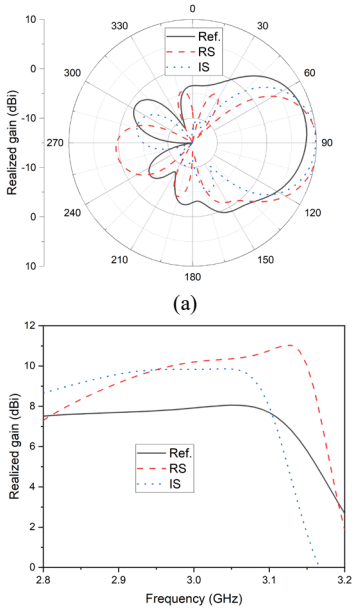

(a)

(b)

Fig. 6. Simulated performance characteristics of all three monopole-based Yagi-Uda antennas with square ground planes. (a) Realized gain patterns in the φ = 0° (xoz) plane at 3.0 GHz. (b) Realized gain along the endfire direction (+x-axis) as a function of the source frequency.

Because the rectangular slots of the RS version are longer than those of IS version, its radiated beam in Fig. 6(a) is clearly narrower, but its backlobe is larger. Moreover, while Fig. 6(b) shows that it also has a higher peak gain at higher frequencies, nevertheless the RS and IS versions have about the same value at the target frequency 3.0 GHz. The back lobe of the RS version is 1.78 dB larger than that of the Ref. antenna. This feature occurs because the beam generated by the Ref. antenna is tilted with respect to the horizontal plane. Consequently, the back-radiated fields are reflected in the ground, thus reducing the backlobe level. Moreover, the IS version requires considerably less transverse space. Consequently, it was selected to form the circular array of 18 monopole-based Yagi-Uda antennas (termed units below) with the I-shaped slot structures illustrated in Fig.7.

The ground plane is now circular rather than rectangular. Its diameter is 374.0 mm (3.74 λ_0). The distance between the reflector element and the center of the ground plane is S0 = 90.0 mm, and the angle between the center lines of any two adjacent units is 20°. Two small metallic rods are located beside the driven dipole to improve the impedance matching as illustrated in Fig. 7(b). The distance between each rod and the corresponding driver is 2.8 mm. The height of each rod is 16.0 mm. The main beam of the array can be scanned to cover the full horizontal plane by exciting different Yagi-Uda units. Furthermore, a few Yagi-Uda units forming a sector can be excited together with the same phase to achieve a high gain.

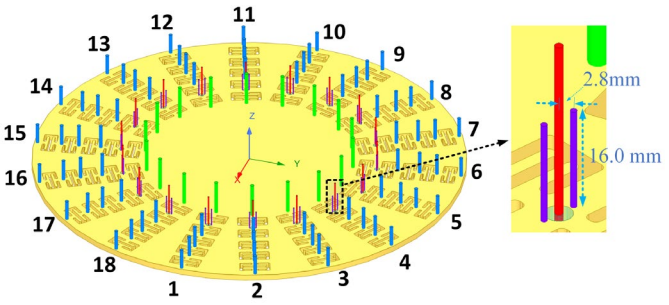

(a) (b)

Fig. 7. Circular array of 18 monopole-based Yagi-Uda antennas with I-shaped slot structures. The diameter of its circular ground disc is 374.0 mm. The angle between any two adjacent elements is 20°.

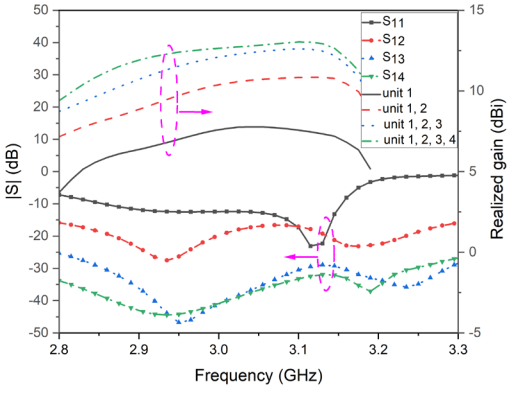

Fig. 8. Magnitude of the S-parameters and the realized gain values of the circular array as functions of the source frequency and the number of active ports.

The simulated magnitude of the S-parameters and the realized gain values for the array are presented in Fig. 8. Because of the symmetry of the array, only the input reflection coefficient of Port 1 is shown along with a comparison of the coupling coefficients between Ports 1 and their adjacent ports – Port 2, Port 3, and Port 4. It is clearly seen that the antenna is matched well to its assumed 50 Ω source with $|S_{11}| \leq -10$ dB between 2.85 and 3.15 GHz, a 10% fractional bandwidth (FBW). The mutual coupling between unit 1 and its adjacent unit – the Yagi-Uda unit excited by Port 2 – is the strongest, but it is less than –15.0 dB over its entire –10.0 dB impedance bandwidth.

The simulated peak realized gain values of the array with different numbers of active units are compared in Fig. 8. When more than one unit is active, they are all excited in phase. These curves show that the total realized gain increases across the entire operating band as more elements become active. In fact, the maximum response occurs when unit 1 – unit 4 are excited in phase. The peak value of the 4-unit case is 12.5 dBi at 3.0 GHz, which is around 5 dB higher than the single active unit case.

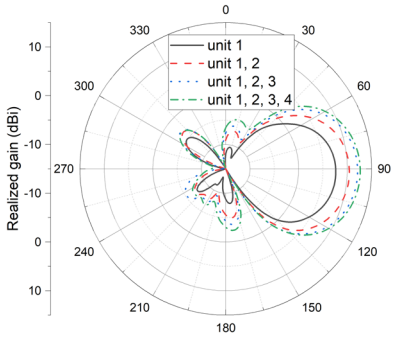

(a) E-plane (θ varies)

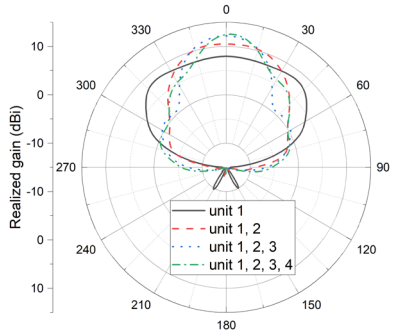

(b) H-plane (ϕ varies)

Fig. 9. Realized gain patterns of the circular Yagi-Uda array with different number of active elements.

The simulated realized gain patterns of the array with different numbers of active units are presented in Fig. 9 in both the E-plane and the H-plane. The peak of the beam in the E-plane (xoz) of each array in Fig. 9(a) is pointed towards the endfire direction, i.e., the beams are no longer elevated. The corresponding realized gain patterns in the H-plane (xoy) are given in Fig. 9(b); they have been manually rotated so that the main beam of each case is centered on the x-axis for comparison purposes. The H-plane realized gain patterns of the array with 4 sequential sets of 4 active units are shown in Fig. 10 to illustrate its beam scanning ability. The beam directions for each sector are 30°, 50°, 70°, and 90°, respectively. A 20º resolution between the beam directions is thus demonstrated, and the gain drop of the overlapping patterns is below 1.6 dB. Other scanning angles to cover a full azimuth plane can be achieved when other sets of units are excited.

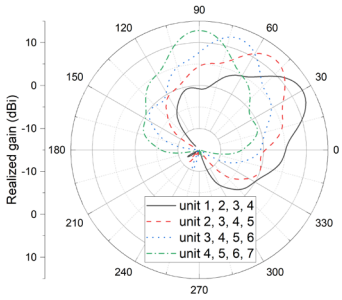

Fig. 10. Realized gain pattern of the array in the xoy plane when its beam is scanned. 30º: units 1–4; 50º: units 2–5; 70º: units 3–6; and 90º: units 4–7.

The developed system and several reported circular arrays of monopoles are compared in TABLE I. It is recognized that in comparison to [6], [8], [10], and [17], our circular array of monopoles with a set of resonant slots introduced into its ground between its active and passive elements provides an innovative approach that redirects the main beam to the horizontal direction, facilitates the steering of it in the azimuthal plane, and realizes a higher peak realized gain.

TABLE I
PERFORMANCE COMPARSION OF CIRCULAR ARRAYS OF MONOPOLES

Ref.	Number of passive units in the circular array	Freq. (GHz)	Peak realized gain of beam (dBi)	Main beam direction in the E-plane	Method to suppress the undesired currents on the ground plane
[6]	5	1.575	6.4	horizontal	Skirted ground
[8]	5	0.9 / 1.9	2.8 / 4	horizontal	Infinite ground
[10]	6	2.4	8.08	9.7° above the ground plane	Skirted ground
[17]	18	2.45	10.0	horizontal	Reflector on top of the array
This work	18	3.0	12.5	horizontal	Ground with resonant slots

IV. Prototype Array and Measured Results

Due to a limited budget, we only fabricated a 60º sector of the whole array, i.e., three Yagi-Uda units, to verify the validity of the developed method. The prototype is shown in Fig. 11. The dimensions of the Yagi-Uda array units are the same as those in Fig. 7 for the IS case. The unit excited by Port 1 is our focus as it has two adjacent elements. This configuration can mimic the units in the whole circular array in Fig. 7. The slots are etched in a 5.0 mm thick, fan-shaped aluminum plate. A 1.0 mm thick solid sector, which has the same shape as the slot-based one, is placed 0.3 λ_0 below the antenna and is grounded. The reflectors and drivers are threaded on the floor from the top of the ground to the bottom. A requisite pair of copper rods was soldered beside each of the driven dipoles. The two plates are supported by 4 Nelon posts. The radius of the inner arc R_{in} is 55.0 mm; the distance from the edge of the sector to the nearest element axis line S is 25.0 mm. This mechanically stable configuration greatly simplified the measurement setup.

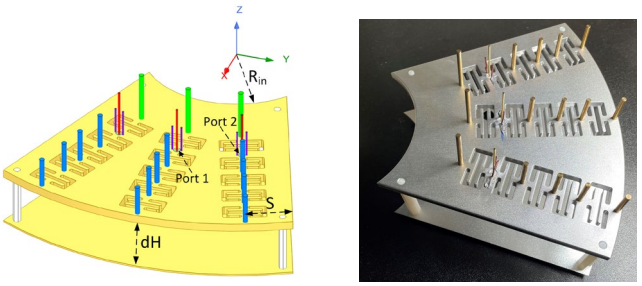

(a) (b)

Fig. 11. Prototype 60º sector of the circular Yagi-Uda array. (a) Model. (b) Photo of the prototype. S = 25.0 mm, R_{in} = 55.0 mm, dH = 30.0 mm.

The simulated and measured S-parameters are shown in Fig. 12. When Port 1 is excited, the other two ports were loaded with a 50 Ω matched impedance. It can be seen that the simulated input reflection coefficients are below –10 dB from 2.9 to 3.15 GHz, and the measured results are below –10.0 dB across this frequency band. The mutual coupling is less than –18.0 dB over the entire band for the simulated and measured systems. Thus, good agreement between the simulated and measured results is demonstrated.

The simulated and measured realized gain patterns in the E- and H-planes for the prototype at different frequencies are compared in Fig. 13. Only vertical polarization components are shown in the figures because of the high polarization purity of the monopole antenna. The cross-polarized values are too small to be included on the given scale. Overall, good agreement is found in these results and the main beams of the E-plane are pointed in the horizontal direction.

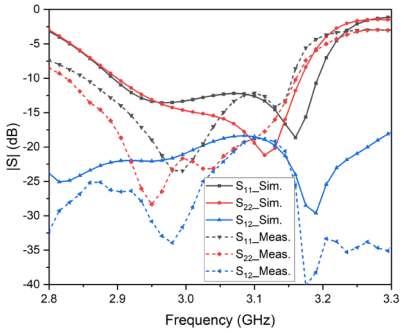

Fig. 12. Simulated and measured S-parameters of the prototype sector.

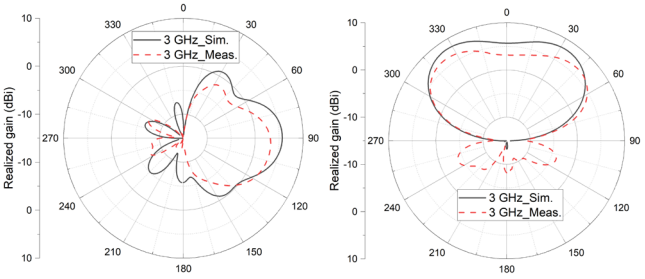

(a) 3.0 GHz, E-plane (b) 3.0 GHz, H-plane

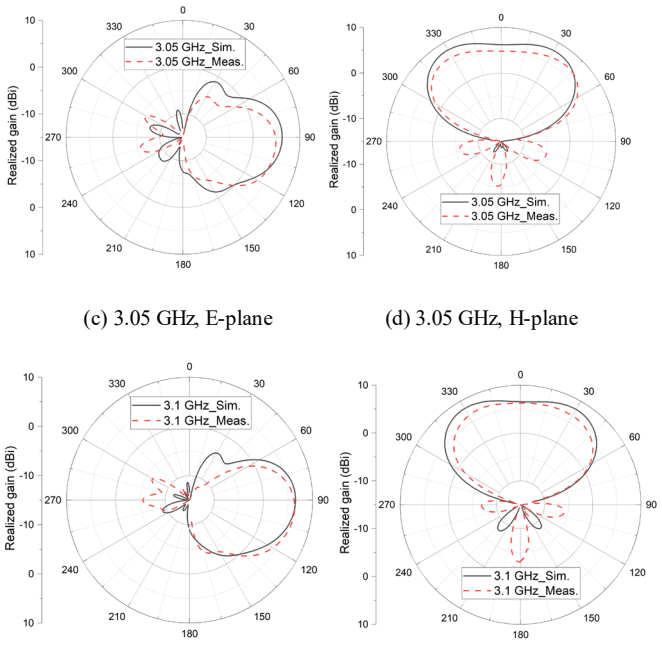

(c) 3.05 GHz, E-plane (d) 3.05 GHz, H-plane

(e) 3.1 GHz, E-plane (f) 3.1 GHz, H-plane

Fig.13. Simulated and measured realized gain patterns of the fabricated prototype sector when it is excited by Port 1 at three freqency points.

Therefore, the technology developed to re-direct the main beam of a monopole-based Yagi-Uda array to the horizontal direction is validated. It is noted that the realized gain patterns of the Yagi-Uda unit excited by Port 1 in the prototype sector are slightly different from those of the single unit (unit 1) of the circular array shown in Fig. 9. These differences occur because the dimensions of the three fabricated units of the sector were optimized in regards to the entire circular array environment, not just as a single unit.

The measured radiation patterns have larger backlobe levels than the simulated ones do. This difference is attributed to inaccuracies in the distance of the antenna from the additional conducting plate that had to be introduced for mounting the antenna in the measurement chamber. Stray currents excited on the long cables present in the measurements also contributed to this difference.

V. Conclusion

The well-known fact that the beam generated by a monopole antenna mounted on a finite ground plane becomes elevated because of the currents it induces on the ground plane was considered. It was demonstrated that by inserting resonant slot structures into the ground plane, this undesirable effect can be suppressed. Monopole-based Yagi-Uda antennas were then developed that have their main beams directed at their endfire direction along the horizontal plane with a realized gain improvement. A circular array of these monopole-based Yagi-Uda antennas was also designed and simulated. By exciting different sectors formed by sets of these Yagi-Uda antennas, full azimuthal beam scanning was achieved. Measurements of a prototype sector of this array confirmed the efficacy of the overall design process. It is anticipated that this innovative circular array with its high realized gain and its ability to have its beam scanned to provide a full 360º coverage of the azimuthal plane will be of practical interest since it can provide multicell coverage to manage the extreme traffic density in many wireless ecosystems.

References

[1] M. Kahar and M. K. Mandal, “A wideband tightly coupled slot antenna for 360° full azimuthal beam steering applications,” *IEEE Trans. Antennas Propag.*, vol. 69, no. 6, pp. 3538-3542, Jun. 2021.

[2] H. Fan, X. Liang, J. Geng, R. Jin and X. Zhou, “Switched multibeam circular array with a reconfigurable network,” *IEEE Trans. Antennas Propag.*, vol. 64, no. 7, pp. 3228-3233, Jul. 2016.

[3] L. Ge, M. Li, Y. Li, H. Wong and K. Luk, “Linearly polarized and circularly polarized wideband dipole antennas with reconfigurable beam direction,” *IEEE Trans. Antennas Propag.*, vol. 66, no. 4, pp. 1747-1755, Apr. 2018.

[4] P. Wang et al., “Beam switching antenna based on a reconfigurable cascaded feeding network,” *IEEE Trans. Antennas Propag.*, vol. 66, no. 2, pp. 627-635, Feb. 2018.

[5] D. V. Thiel and S. Smith, Switched parasitic antennas for cellular communications. Boston, MA: Artech House, 2002.

[6] R. Schlub and D. V. Thiel, “Switched parasitic antenna on a finite ground plane with conductive sleeve,” *IEEE Trans. Antennas Propag.*, vol. 52, no. 5, pp. 1343-1347, May 2004.

[7] S. L. Preston, D. V. Thiel, and J. W. Lu, “A multibeam antenna using switched parasitic and switched active elements for space-division multiple access applications,” *IEICE Trans. Commun*., vol. 82-C, pp. 1202–1210, July 1999.

[8] R. Schlub, D. V. Thiel, J. W. Lu, and S. G. O’Keefe, “Dual-band six element switched parasitic array for smart antenna cellular communications systems,” *Electron. Lett.*, vol. 36, no. 16, pp. 1342–1343, 2000.

[9] L. Zhang, S. Gao, Q. Luo, P. R. Young and Q. Li, “Planar ultrathin small beam-switching antenna,” *IEEE Trans. Antennas Propag.*, vol. 64, no. 12, pp. 5054-5063, Dec. 2016.

[10] R. Schlub, Junwei Lu and T. Ohira, “Seven-element ground skirt monopole ESPAR antenna design from a genetic algorithm and the finite element method,” *IEEE Trans. Antennas Propag.*, vol. 51, no. 11, pp. 3033-3039, Nov. 2003.

[11] C. Gu et al., “3-D coverage beam-scanning antenna using feed array and active frequency-selective surface,” *IEEE Trans. Antennas Propag.*, vol. 65, no. 11, pp. 5862-5870, Nov. 2017.

[12] L. Zhang, Q. Wu and T. A. Denidni, “Electronically radiation pattern steerable antennas using active frequency selective surfaces,” *IEEE Trans. Antennas Propag.*, vol. 61, no. 12, pp. 6000-6007, Dec. 2013.

[13] B. Liang, B. Sanz-Izquierdo, E. A. Parker and J. C. Batchelor, “Cylindrical slot FSS configuration for beam-switching applications,” *IEEE Trans. Antennas Propag.*, vol. 63, no. 1, pp. 166-173, Jan. 2015.

[14] Z. L. Ma and C. H. Chan, “A novel surface-wave-based high-impedance surface multibeam antenna with full azimuth coverage,” *IEEE Trans. Antennas Propag.*, vol. 65, no. 4, pp. 1579-1588, Apr. 2017.

[15] A. Sarkar and S. Lim, “Annular surface plasmon polariton-based frequency-scanning leaky-wave antenna for full azimuth coverage,” *IEEE Trans. Antennas Propag.,* accepted.

[16] T. Maruyama, K. Uehara and K. Kagoshima, “Analysis and design of multi-sector monopole Yagi-Uda array mounted on a ground plane using moment method,” *1996 Third International Conference on Computation in Electromagnetics (Conf. Publ. No. 420)*, 1996.

[17] M. D. Migliore and D. Pinchera, “Correction of beam direction in adaptive parasitic monopole arrays using a truncated cone structure,” *IEEE Antennas Wireless Propag. Lett.*, vol. 11, pp. 1486-1488, 2012.

[18] Thiel, D. V. “Optimised slot reradiation to modify foreground reflection into an array,” *Proceedings of the Institution of Electrical Engineers.* vol. 120. no. 9, pp.962-964, Sep. 1973.

[19] Z. Liang, Y. Li, J. Liu, S. Y. Zheng and Y. Long, “Microstrip magnetic monopole endfire array antenna with vertical polarization,” *IEEE Trans. Antennas Propag.*, vol. 64, no. 10, pp. 4208- 4217, Oct. 2016.

[20] N. Honma, T. Seki, K. Nishikawa, K. Tsunekawa and K. Sawaya, “Compact six-sector antenna employing three intersecting dual-beam microstrip Yagi-Uda arrays with common director,” *IEEE Trans. Antennas Propag.*, vol. 54, no. 11, pp. 3055-3062, Nov. 2006.

[21] FEKO. [Online]. Available: https://altairhyperworks.com.

[22] Balanis, Constantine A. Antenna theory: Analysis and design. John wiley & sons, 2015.

[23] HFSS. [Online]. Available: https://www.ansys.com.